

A New Approach to Image Denoising based on Wiener-LMMSE Scheme

Abhinandan Kalita, Md. Sajjad Hossain ,Kandarpa Kumar Sarma
Department of Electronics & Communication Engineering
Gauhati University
Guwahati, Assam, India

ABSTRACT

Several noise removal techniques have proven their worth in image processing applications. After an overview of some image denoising approaches, we introduce a LMMSE-based denoising technique with wavelet multiscale model and wiener filter in spatial domain. This proposed denoising technique stands out prominent in terms of SNR, MSE and PSNR compared to some more denoising techniques (also proposed in this paper). The Overcomplete Wavelet Expansion (OWE) which is also employed, provides better result compared to Orthogonal Wavelet Transform (OWT). Moreover, some fine details of the image such as edges, curves etc. is preserved using the LMMSE rule.

Keywords

Denoising, discrete wavelet transform (DWT), wiener filter, overcomplete wavelet expansion (OWE), multiscale LMMSE, mean square error (MSE), and peak signal to noise ratio (PSNR).

1. INTRODUCTION

Images are often corrupted with noise during acquisition, transmission, and retrieval from storage media. Noise corrupts both images and videos [1]. The purpose of the denoising algorithm is to remove such noise. Image denoising is needed because a noisy image is not pleasant to view. In addition, some fine details in the image may be confused with the noise or vice-versa. Many image-processing algorithms such as pattern recognition need a clean image to work effectively. Random and uncorrelated noise samples are not compressible. Such concerns underline the importance of denoising in image and video processing. Images are affected by different types of noise. Denoising of natural images corrupted by noise using wavelet techniques is very effective because of its ability to capture the energy of a signal in few energy transform values. The wavelet denoising scheme thresholds the wavelet coefficients arising from the wavelet transform. The problem of image denoising can be summarized as follows [2]: let $A(i, j)$ be the noise-free image and $B(i, j)$ be the image corrupted with noise $Z(i, j)$, then

$$B(i, j) = A(i, j) + \sigma * Z(i, j) \quad (1)$$

where σ is the noise variance. In the wavelet domain, the problem can be formulated as

$$Y(i, j) = X(i, j) + W(i, j) \quad (2)$$

where $Y(i, j)$ is noisy wavelet coefficient, $X(i, j)$ is true coefficient and $W(i, j)$ is noise. For the noise deduction purpose, wavelet filters have two properties. Firstly, wavelet filter is capable of extracting the signal information from the noisy wavelet coefficients and secondly, interscale image wavelet coefficients distribution is effectively close to mutually Gaussian distribution [when the distribution is jointly Gaussian, LMMSE is equal to minimum mean square-error estimation (MMSE)]. In this paper, different denoising techniques have been proposed. Out of the models proposed, the wiener filter plus LMMSE-based denoising technique with wavelet multiscale model turns out to be the best in terms of three parameters SNR (signal to noise ratio), MSE (mean square error) and PSNR (peak signal to noise ratio).

2. THEORETICAL BACKGROUND

2.1 Wavelet Transform

Let us take an N by N image. In the decomposition process, the image is high and low-pass filtered along the rows and the results of each filter are down-sampled by two. Those two sub-signals correspond to the high and low frequency components along the rows and are each of size N/2. Then each of these sub-signals is again high and low-pass filtered, along the column data. The results are again down-sampled by two. As a result the original data is split into four sub-images each of size N/2 by N/2 containing information from different frequency components. The LL subband is the result of low-pass filtering both the rows and columns and it contains a rough description of the image as such. Hence, the LL subband is also called the approximation subband. The HH subband is high-pass filtered in both directions and contains the high-frequency components along the diagonals as well. The HL and LH images are the result of low-pass filtering in one direction and high-pass filtering in another direction. LH contains mostly the vertical detail information that corresponds to horizontal edges. HL represents the horizontal detail information from the vertical edges. All three subbands HL, LH and HH are called the detail subbands, because they add the high-frequency detail to the approximation image. In the composition process, the information from the four sub-images is up-sampled and then filtered with the corresponding inverse filters along the columns. The two results that belong together are added and then again up-sampled and filtered with the corresponding inverse filters. The result of the last step is added together in order to get the original image again. There is no loss of information when the image is decomposed and then composed again at full precision [3].

Three performance measures [4] [5] SNR, MSE and PSNR are given as:

$$SNR = 10 * \log_{10} \frac{\text{var}(I)}{\text{var}(e)} \quad (3)$$

where I is the original image and e is the error.

$$MSE = \frac{1}{m * n} * \sum_{i=0}^{m-1} \sum_{j=0}^{n-1} \|I(i, j) - K(i, j)\|^2 \quad (4)$$

$$PSNR = 10 * \log_{10} \frac{MAX_I^2}{MSE} \quad (5)$$

where I and K are the original and noisy (denoised) images, respectively. MAX_I is the maximum possible pixel value of the image.

2.2 Bayesian Thresholding

It refers to the concept of selecting different threshold values for different subbands under consideration. The BayesShrink [6] rule uses a Bayesian mathematical framework for images to derive subband dependent thresholds that are nearly optimal for soft thresholding. The observation model is, $Y = X + W$, with X and W independent of each other, hence

$$\sigma_y^2 = \sigma_x^2 + \sigma^2 \quad (6)$$

where σ_y^2 = variance of Y. Since Y is modeled as zero mean, σ_y^2 can be found empirically by

$$\sigma_y^2 = \frac{1}{n^2} * \sum_{i,j=1}^n (Y_{i,j}^2), \quad (7)$$

where $n*n$ is the size of the subband under consideration.

Thus,
$$T_B(\sigma_x) = \frac{\sigma^2}{\sigma_x} \quad (8)$$

where $\sigma_x = \sqrt{\max(\sigma_y^2 - \sigma^2, 0)}$. In the case that $\sigma^2 \geq \sigma_y^2$, σ_x is taken to be 0. That is, $T_B(\sigma_x)$ is ∞ , or, in practice, $T_B(\sigma_x) = \max(\text{abs}(Y_{i,j}))$ and all coefficients are set to 0. This happens at times when σ is large. Hence, we refer this method as BayesShrink which performs soft thresholding, with the data driven, subband dependent threshold [7].

2.3 Median Filter

The median filter is a nonlinear digital filtering technique, often used to remove noise. Such noise reduction is a typical pre-processing step to improve the results of later processing (for example, edge detection on an image). Median filtering is very widely used in digital image processing because, under certain conditions, it preserves edges while removing noise. It

is more effective method for removing salt and paper noise [8]. It is performed by taking the magnitude of all of the vectors within a mask and sorted according to the magnitudes. The median magnitude of the pixel is used to restore the pixel studied. The median of a set is more dynamic with respect to the presence of noise. The median filter is expressed by

$$MF(x_1, \dots, x_N) = \text{median}(\|x_1\|^2, \dots, \|x_N\|^2) \quad (9)$$

2.4 Wiener Filter

Wiener filter is an optimum filter whose purpose is to reduce the amount of noise present in a signal by comparison with an estimation of the desired noiseless signal. The main goal of Wiener filter is to minimize the mean square error [8]. It is capable of handling both the degradation function as well as noise. The Fourier domain of the Wiener filter is expressed by

$$G(u, v) = \frac{H^*(u, v)}{|H(u, v)|^2 P_s(u, v) + P_n(u, v)} \quad (10)$$

Where, $H(u, v)$ = Degradation function

$H^*(u, v)$ = Complex conjugate of degradation function

$P_n(u, v)$ = Power Spectral Density of Noise

$P_s(u, v)$ = Power Spectral Density of non-degraded image

2.5 Overcomplete Wavelet Expansion

Orthogonal Wavelet Transform (OWT) sometimes cause visual artifacts in threshold-based noise removal [9 – 20] and it has been observed that the OWE obtain better results in noise repression and artifacts reduction. Instead of down sampling of wavelet coefficients in OWT, the restored image by OWE is an average of several circularly shifted noise removed adaptations of the same signal by OWT by which the additive white Gaussian noise is well suppressed [21] [22].

2.6 Multiscale LMMSE Interscale Model

Let us assume that the original image f corrupted with additive Gaussian white noise ϵ , is defined as

$$I = f + \epsilon \quad (11)$$

Where $\epsilon \in N(0, \sigma^2)$, Applying the OWE to the noisy signal at scale k yields

$$w_k = x_k + v_k \quad (12)$$

Where, w_k is a coefficient at scale k , x_k and v_k are the expansions of f and ϵ respectively.

Instead of using universal soft and hard thresholding, LMMSE method is applied. Hence the LMMSE of x_k is given by, since $x_k \in N(0, \sigma_{x_k}^2)$ and $v_k \in N(0, \sigma_k^2)$

$$\widehat{x}_k = c' \square w_k \quad (13)$$

With
$$c = \frac{\sigma_{x_k}^2}{\sigma_{x_k}^2 + \sigma_k^2} \quad (14)$$

The expression w_{k+1}^D of is expressed in the form of

$$\sigma_k = \|L_{k-1}\| \sigma w_{k+1}^D = S_0 * L_k^D \quad (15)$$

Where * is the convolution operator and filter L_k^D is

$$L_k^D = H_0 * H_0' * \dots * H_{k-1} * H_{k-1}' * G_k * G_k' \quad (16)$$

Similarly for horizontal and vertical direction, we have

$$w_{k+1}^H = S_0 * L_k^H \text{ and } w_{k+1}^V = S_0 * L_k^V \quad (17)$$

Where

$$L_k^H = H_0 * H_0' * \dots * H_{k-1} * H_{k-1}' * G_k * G_k' \text{ And}$$

$$L_k^V = H_0 * H_0' * \dots * H_{k-1} * H_{k-1}' * G_k * G_k' \quad (18)$$

Noise standard deviation of v_k at scale k in a direction (horizontal, vertical or diagonal) is

$$\sigma_{k-1} = \|L_{k-1}\| \sigma \quad (19)$$

Where L_{k-1} is the corresponding filter. The standard deviation of σ_{x_k} noiseless image is x_k estimated as

$$\sigma_{x_k}^2 = \sigma_{w_k}^2 - \sigma_k^2 \quad (20)$$

With,
$$\sigma_{w_k}^2 = \frac{1}{MN} \sum_{m=1}^M \sum_{n=1}^N w_k^2(m, n) \quad (21)$$

Where, M, N is the numbers of input image rows and columns.

The LMMSE-based wavelet noise removal system proposed in [23] [24] obtained better results. These two systems exploited the wavelet interscale dependencies. Therefore, to accomplish an interscale wavelet model which is based on LMMSE, the wavelet adjacent scales are strongly correlated and these interscale dependencies can be exploited for better noise removal results. The wavelet based represented images

are similar across scales and especially among the adjacent scales. In wavelet domain, the noise level decrease swiftly along scales, while signal structures are strengthened with scale rising. Thus coarser scale information is being used to recover finer scale estimation. When the input image is decomposed into k scales, then scale k is strongly correlated with scale $k+1$, but its correlations with scales $k+2, k+3, \dots$ decreases rapidly.

Now, we accumulate the points with the same orientation at scales k and $k+1$ as a vector

$$\overline{w_k(m, n)} = [w_k(m, n), w_{k+1}(m, n)]^T \quad (22)$$

$$\overline{w_k} = \overline{x_k} + \overline{v_k} \quad (23)$$

Where,

$$\overline{x_k(m, n)} = [x_k(m, n), x_{k+1}(m, n)]^T$$

$$\overline{v_k(m, n)} = [v_k(m, n), v_{k+1}(m, n)]^T \quad (24)$$

The LMMSE of $\overline{x_k}$ is expressed by

$$\widehat{x} = P_k (P_k + R_k)^{-1} \overline{w_k} \quad (25)$$

Here the covariance matrices of x_k and v_k are represented by

$$P_k \text{ and } R_k$$

$$P_k = E[\overline{x_k} \overline{x_k}^T] \quad (26)$$

$$R_k = E[\overline{v_k} \overline{v_k}^T] \quad (27)$$

The correlation coefficient value is expressed by,

$$\rho_{k, k+1} = \frac{\sqrt{\sum_l \sum_K L_k(r, s) L_k(r, s)}}{\|L_{k-1}\| \|L_k\|} \quad (28)$$

v_k and v_{k+1} represent the joint Gaussian distribution function. So, the density is given by,

$$\rho(v_k, v_{k+1}) = \frac{1}{2\pi\sigma_k\sigma_{k+1}\sqrt{1-\rho_{k,k+1}^2}} * e^{-\frac{1}{2(1-\rho_{k,k+1}^2)}\left[\frac{v_k^2}{\sigma_k^2} - \frac{2\rho_{k,k+1}v_kv_{k+1}}{\sigma_k\sigma_{k+1}} + \frac{v_{k+1}^2}{\sigma_{k+1}^2}\right]} \quad (29)$$

The probable value is given by,

$$E[v_kv_{k+1}] = \rho_k\rho_{k+1}\sigma_k\sigma_{k+1} \quad (30)$$

$$E[x_r x_s] \approx E[w_r w_s] - E[v_r v_s] \quad (31)$$

Where, r and s represents k and $k+1$ respectively

$$E[w_r w_s] = \frac{1}{MN} \sum_{m=1}^M \sum_{n=1}^N w_r(m, n).w_s(m, n) \quad (32)$$

3. DESIGN AND IMPLEMENTATION OF THE PROPOSED DENOISING TECHNIQUE

In this work, the major focus is to design a technique that provides better denoised output compared to the following noise removal techniques in terms of SNR, MSE and PSNR. Fig 1 shows a Wiener-Bayesian wavelet based image denoising technique. In this model, wiener filter is used for the pre-processing stage and the filtered output is fed to the Bayesian network for further denoising. Similarly, fig 2 shows a Median-Bayesian wavelet based image denoising technique. Fig 3 shows a Median-LMMSE based denoising technique

with wavelet multiscale model. Fig 4 shows the proposed model.

4. EXPERIMENTAL RESULTS AND COMPARISONS

Table 1. Comparison of different denoising schemes (Random Noise Variance $\sigma=25$)

Denoising Schemes	Input SNR (dB)	Output SNR (dB)	MSE	PSNR (O/N) dB	PSNR (O/D) dB
WB	14.5896	16.5759	395.58	20.174	22.158
MB	14.5896	16.72	382.68	20.141	22.302
MLMMSE	14.5896	18.4511	256.87	20.176	24.0335
Proposed	14.5896	20.159	173.35	20.164	25.7414

Table 2. Comparison of different denoising schemes (Random Noise Variance $\sigma=30$)

Denoising Schemes	Input SNR (dB)	Output SNR (dB)	MSE	PSNR (O/N) dB	PSNR (O/D) dB
WB	13.006	16.413	410.63	18.547	21.99
MB	13.006	16.540	398.84	18.574	22.12
MLMMSE	13.006	17.977	286.48	18.607	23.56
Proposed	13.006	19.446	204.27	18.618	25.03

Table 3. Comparison of different denoising schemes (Random Noise Variance $\sigma=35$)

Denoising Schemes	Input SNR (dB)	Output SNR (dB)	MSE	PSNR (O/N) dB	PSNR (O/D) dB
WB	11.667	16.265	424.94	17.227	21.84
MB	11.667	16.396	412.27	17.261	21.98
MLMMSE	11.667	17.865	293.98	17.286	23.44
Proposed	11.667	18.949	229.04	17.251	24.53

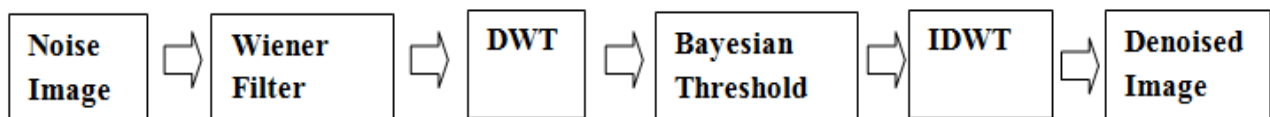


Fig 1: Wiener-Bayesian (WB) Model

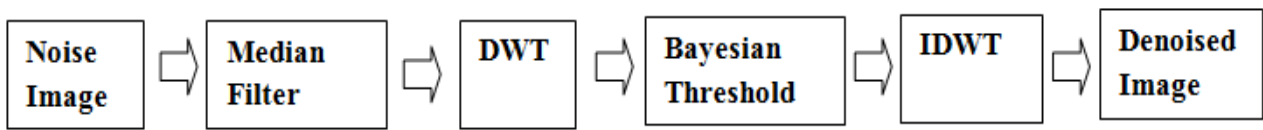


Fig 2: Median-Bayesian (MB) Model

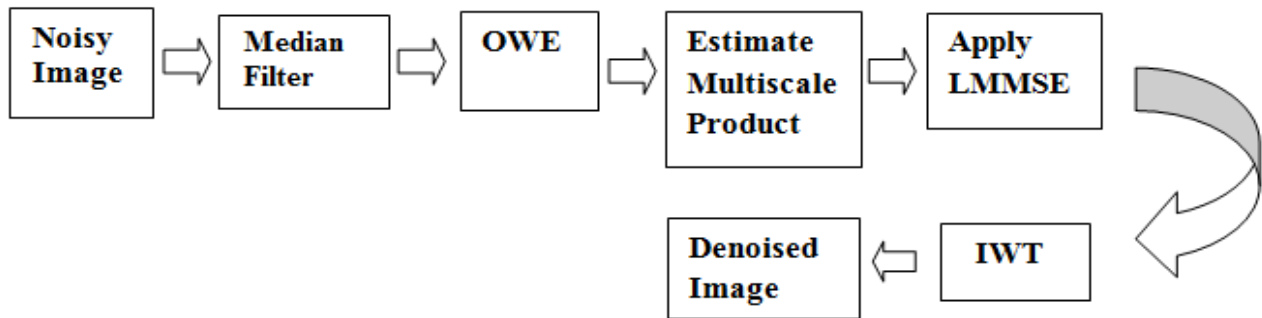


Fig 3: Median-LMMSE (MLMMSE) Model

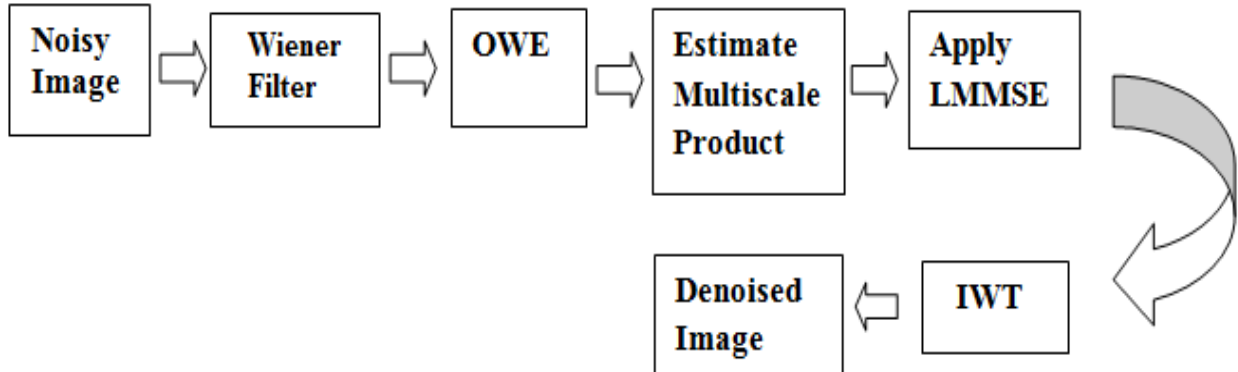


Fig 4: Wiener-LMMSE Model (Proposed)

Table 4. Performance Improvement of the proposed model compared to the other three models (Random Noise Variance $\sigma = 25$) in %

Models	SNR	MSE	PSNR
WB	21.61	56.67	16.17
MB	20.56	54.69	15.42
MLMMSE	9.26	32.51	7.12

Table 5. Performance Improvement of the proposed model compared to the other three models (Random Noise Variance $\sigma = 30$) in %

Models	SNR	MSE	PSNR
WB	18.48	50.25	13.8
MB	17.57	48.78	13.13
MLMMSE	8.17	28.69	6.23

Table 6. Performance Improvement of the proposed model compared to the other three models (Random Noise Variance $\sigma = 35$) in %

Models	SNR	MSE	PSNR
WB	16.5	46.1	12.28
MB	15.56	44.4	11.6
MLMMSE	6.06	22.08	4.61



Fig 5: Denoised Images using various Denoising Models ($\sigma = 25$)

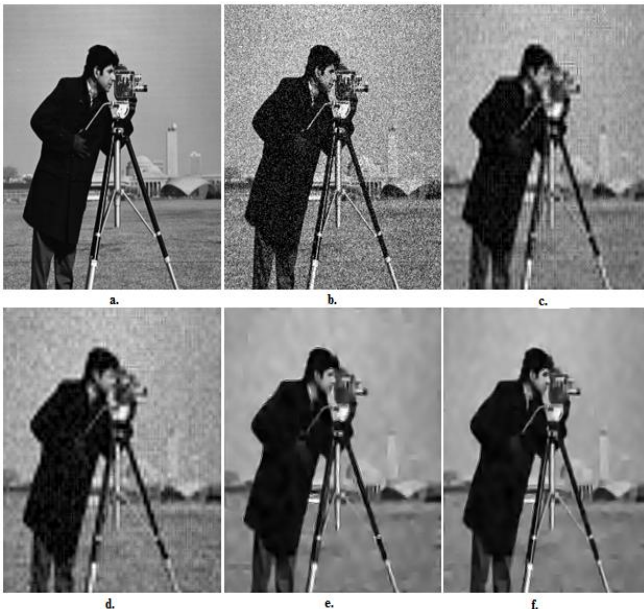


Fig 6: Denoised Images using various Denoising Models ($\sigma = 30$)



Fig 7: Denoised Images using various Denoising Models ($\sigma = 35$)

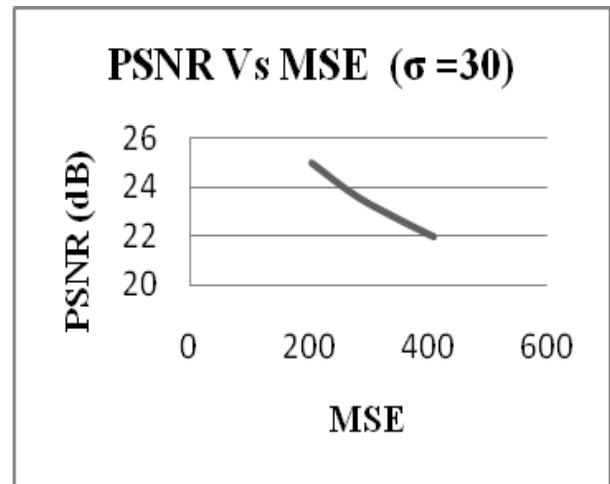


Fig 8: PSNR vs. MSE Graph ($\sigma = 30$)

MSE, SNR and PSNR values are calculated for different combinations separately. Fig 5 shows a set of denoised images using different denoising models for noise variance of 25. (a.) is the original image; (b.) is the noise corrupted with random noise; (c.) is the result of WB Model; (d.) is the result of MB Model; (e.) is the result of MLMMSE Model; and (f.) is the denoised output of the proposed model. Similarly, fig 6 and fig 7 shows a set of denoised images for noise variance 30 and 35. Fig 8 shows a graph for PSNR vs. MSE. Table I, II and III shows a set of results obtained from denoising operations carried out using different models. Table IV, V and VI shows the performance improvement of the proposed model compared to the other three models.

5. CONCLUSION

From experimental results, it can be concluded that the proposed denoising technique leads to fairly satisfactory results as far as denoising of image corrupted with random noise is concerned. This work can be further enhanced to denoise the other type of images, as well, like RGB, Indexed and Binary images. Use of AI techniques will lead to the optimal solution directly, with more efficiency and less tedious work.

6. REFERENCES

- [1] R.E.Woods, R.C.Gonzalez, "Digital Image Processing", Pearson Prentice Hall, 3rd ed., 2009.
- [2] G.Y.Chen, T. D. Bui and A. Krzyzak, "Image denoising using neighbouring wavelet coefficients", *IEEE*, pp. II (917-920), *ICASSP*, 2004.
- [3] Michel Misiti, Yves Misiti, Georges Oppenheim, Jean-Michel Poggi, "Wavelet Toolbox for use with MATLAB", User's guide, version 2.1, pp. 1-37.
- [4] Aleksandra Pizurica, Wilfried Philips, Ignace Lemahieu and Marc Acheroy, "A Versatile Wavelet Domain Noise Filtration Technique for Medical Imaging", *IEEE transactions on medical imaging*, vol. 22, no. 3, pp. 323-331, March 2003.
- [5] S.Sudha, G.R.Suresh, R.Sukanesh, "Wavelet Based Image Denoising using Adaptive Thresholding", *International Conference on Computational Intelligence and Multimedia Applications*, pp. 296-300, 2007.
- [6] N.G.Resmi, K.P.Soman, K.I.Ramachandran, "Insight into wavelets from theory to practice", PHI, 3rd ed., New Delhi, 2011
- [7] S.Grace Chang, Bin Yu and Martin Vetterli, "Adaptive Wavelet Thresholding for Image Denoising and Compression", *IEEE transactions on image processing*, vol. 9, no. 9, pp. 1532-1546, September 2000.
- [8] S. Kumar, P. Kumar, M.Gupta, A. K. Nagawat "Performance Comparison of Median and Wiener Filter in Image De-noising" *International Journal of Computer Applications (0975 – 8887) Volume 12– No.4, November 2010.*
- [9] D. L. Donoho and I. M. Johnstone, "Ideal spatial adaptation by wavelet shrinkage," *Biometrika*, vol. 81, no. 3, pp. 425–455, 1994.
- [10] D. L. Donoho, I. M. Johnstone, G. Kerkyacharian, and D. Picard, "Wavelet shrinkage: Asymptopia?," *J. Roy. Statist. Assoc. B*, vol. 57, no. 2, pp. 301–369, 1995.
- [11] S. G. Chang, B. Yu, and M. Vetterli, "Adaptive wavelet thresholding for image denoising and compression," *IEEE Trans. Image Process.*, vol. 9, no. 9, pp. 1532–1546, Sep. 2000.
- [12] J. Portilla, V. Strela, M. J. Wainwright, and E. P. Simoncelli, "Image denoising using scale mixtures of Gaussians in the wavelet domain", *IEEE Trans. Image Process.*, vol. 12, no. 11, pp. 1338–1351, Nov. 2003.
- [13] Pizurica and W. Philips, "Estimating the probability of the presence of a signal of interest in multiresolution single- and multiband image denoising" *IEEE Trans. Image Process.*, vol. 15, no. 3, pp. 654–665, Mar. 2006.
- [14] L. Sendur and I. W. Selesnick, "Bivariate shrinkage functions for wavelet-based denoising exploiting interscale dependency," *IEEE Trans. Signal Process.* vol. 50, no. 11, pp. 2744–2756, Nov. 2002.
- [15] L. Sendur and I. W. "Selesnick, Bivariate shrinkage with local variance estimation," *IEEE Signal Process. Lett.*, vol. 9, no. 12, pp. 438–441, Dec. 2002.
- [16] F. Luisier, T. Blu, and M. Unser, "A new sure approach to image denoising: Inter-scale orthonormal wavelet thresholding," *IEEE Trans. Image Process.*, vol. 16, no. 3, pp. 593–606, Mar. 2007.
- [17] D.L.Donoho, "Denoising and soft thresholding," *IEEE Transactions. Information. Theory*, Vol.41, PP.613-627, 1995.
- [18] D.L.Donpho, and I.M.Johnstone, "Adaptive to unknown smoothness via wavelet shrinkage", *Journal of American statistical ASSOC.*, VOL.90, NO.90, PP.1200-1224, 1995.
- [19] D.L.Donpho, and I.M.Johnstone, "Ideal spatial adaptation via wavelet shrinkage", *Biometrika*, VOL.81, PP.425-455, 1994.
- [20] I. Pitas and A.N.Venetsanopoulos, "Nonlinear Digital Filters: Principles and applications", Boston, MA: Kluwer. 1990.
- [21] J. Liu and P. Moulin, "Information-theoretic analysis of interscale and intrascale dependencies between image wavelet coefficients," *IEEE Trans. Image Process.*, vol. 10, no. 11, pp. 1647–1658, Nov. 2001.
- [22] Lei Zhang, Paul Bao., "Multiscale LMMSE-Based Image Denoising With Optimal Wavelet Selection," *IEEE Transactions On Circuits And Systems*, vol. 15, NO. 4, Apr, 2005.
- [23] M. K. Mihçak, I. Kozintsev, K. Ramchandran, and P. Moulin, "Low complexity image denoising based on statistical modeling of wavelet coefficients," *IEEE Signal Process. Lett.*, vol. 6, no. 12, pp. 300–303, Dec. 1999.
- [24] X. Li and M. Orchard, "Spatially adaptive image denoising under overcomplete expansion," in *Int. Conf. Image Process.*, Vancouver, Canada, pp. 300–303, Sep. 2000.